

# ANALYTICAL MODEL OF CRYOGENIC HYDROGEN RELEASES

Zhang, J.X.<sup>1</sup>, Ba, Q.X.<sup>2</sup>, Xiao, J.S.<sup>3</sup>, Christopher, D.M.<sup>4</sup>, Liu, Y.<sup>5</sup>, Yao, C.Y.<sup>6</sup> and Li, X.F.<sup>7,\*</sup>

<sup>1</sup>Institute of Thermal Science and Technology (Institute for Advanced Technology), Shandong University, Jingshi Road, Jinan, 250061, China, [jiaxinz1998@163.com](mailto:jiaxinz1998@163.com)

<sup>2</sup>School of Mechanical Engineering, Shandong University, Jingshi Road, Jinan, 250061, China, [qingxin90113@126.com](mailto:qingxin90113@126.com)

<sup>3</sup>Hubei Research Center for New Energy & Intelligent Connected Vehicle, School of Automotive Engineering, Wuhan University of Technology, Luoshi Road, Wuhan, 430070, China,

[Jinsheng.Xiao@uqtr.ca](mailto:Jinsheng.Xiao@uqtr.ca)

<sup>4</sup>Key Laboratory of Thermal Science and Power Engineering of Ministry of Education, Tsinghua University, Hai Dian, Beijing, 100084, China, [dmc@tsinghua.edu.cn](mailto:dmc@tsinghua.edu.cn)

<sup>5</sup>Institute of Thermal Science and Technology (Institute for Advanced Technology), Shandong University, Jingshi Road, Jinan, 250061, China, [liuyue10091@163.com](mailto:liuyue10091@163.com)

<sup>6</sup>Institute of Thermal Science and Technology (Institute for Advanced Technology), Shandong University, Jingshi Road, Jinan, 250061, China, [yaochenyi0417@163.com](mailto:yaochenyi0417@163.com)

<sup>7</sup>Institute of Thermal Science and Technology (Institute for Advanced Technology), Shandong University, Jingshi Road, Jinan, 250061, China, [lixf@email.sdu.edu.cn](mailto:lixf@email.sdu.edu.cn)

## ABSTRACT

Hydrogen is one of the most promising alternative sources to relieve the energy crisis and environmental pollution. Hydrogen can be stored as cryogenic compressed hydrogen (CCH<sub>2</sub>) to achieve high volumetric energy densities. Reliable safety codes and standards are needed for hydrogen production, delivery, and storage to promote hydrogen commercialization. Unintended hydrogen releases from cryogenic storage systems are potential accident scenarios that are of great interest for updating safety codes and standards. This study investigated the behavior of CCH<sub>2</sub> releases and dispersion. The extremely low-temperature CCH<sub>2</sub> jets can cause condensation of the air components, including water vapor, nitrogen and oxygen. An integral model considering the condensation effects was developed to predict the CCH<sub>2</sub> jet trajectories and concentration distributions. The thermophysical properties were obtained from the COOLPROP database. The model divides the CCH<sub>2</sub> jet into the underexpanded, initial entrainment and heating, flow establishment and established flow zones. The condensation effects on the heat transfer and flow were included in the initial entrainment and heating zones. The empirical coefficients in the integral model were then modified based on measured concentration results. Finally, the analytical model predictions are shown to compare well with measured data to verify the model accuracy. The present study can be used to develop quantitative risk assessment models and update safety codes and standards for cryogenic hydrogen facilities.

Keywords: Cryogenic compressed hydrogen; Condensation; Hydrogen release; Integral model

## 1.0 INTRODUCTION

Hydrogen energy has been regarded as a promising alternative to fossil fuels due to its cleanliness and renewability, which can potentially help address environmental pollution and energy crisis issues [1,2]. Hydrogen energy is expected to play a significant role in the transition to a low-carbon economy. Many countries have established targets and policies to promote hydrogen energy development [3-5].

Hydrogen is a highly flammable gas, posing safety risks to its utilization, storage, and transportation. Hydrogen safety is critical to increasing public awareness and promoting the development and application of hydrogen energy technology. Hydrogen may quickly disperse and form an explosive mixture with air after leakage, creating a potential fire or explosion hazard. Therefore, the hydrogen leakage behavior is a major concern in hydrogen safety research.

Hydrogen releases from high-pressure sources will lead to underexpanded jets. Many experimental and CFD studies have analyzed the concentration and velocity distributions of underexpanded hydrogen jets [6-9]. The hydrogen jet parameters are self-similar in the momentum-dominated region. The jet centerline concentration and velocity distributions follow the hyperbolic decay law and the radial concentration and velocity distributions follow Gaussian curves.

An integral model for low-pressure leakage, which was originally developed for pollutant diffusions and distributions [10,11], has been used to model subsonic hydrogen jets [12-14]. The integral model includes the mass, momentum and energy conservation equations, and the jet parameter distribution characteristics. However, the integral model cannot be directly used to calculate underexpanded jets due to the complex shock structure near nozzle outlets. Several notional nozzle models have been developed by Birch et al. [15,16], Ewan and Moodie [17], Yuceil and Otugen [18], and Molkov et al. [19] to provide appropriate boundary conditions for the integral model, and then the integral model is available for the underexpanded hydrogen jets. Li et al. [20] determined the values of key model parameters by comparing with the experimental data. The integral model with corrected parameters then predicted the room-temperature underexpanded hydrogen jets quickly and accurately.

Cryogenic compressed hydrogen ( $CcH_2$ ) with its higher density can be a more efficient and economical method for storage and transport compared with room-temperature hydrogen. A few studies have focused on the measurement and simulation of  $CcH_2$  jets to analyze the concentration, temperature and velocity distributions [21-25]. Air components, including nitrogen, oxygen and water vapor, will condense in the initial entrainment and heating zone of cryogenic compressed hydrogen jets, which will affect the hydrogen jet diffusions. However, the integral model did not take into account the condensation phase transition effects.

In the present study, an integral model considering the condensation effects was developed to predict the  $CcH_2$  jet concentration distributions. The  $CcH_2$  jet was divided into the underexpanded flow, initial entrainment and heating, flow establishment and established flow zones. The condensation effects on the heat transfer and flow were included in the initial entrainment and heating zones. The analytical model was then validated by comparisons to measured data.

## **2.0 MODEL DESCRIPTIONS**

### **2.1 The integral model**

Based on Gebhart's integral turbulent plume model [11], Winters and Houf [6, 12] developed a one-order plume model for describing hydrogen jets. The model has now been incorporated into the HyRAM toolkit [26], a hydrogen safety risk assessment software developed by Sandia National Laboratory. In Winters and Houf's work, the jet flow field is divided into four zones: (I) underexpanded zone, (II) initial entrainment and heating zone, (III) flow establishment zone, and (IV) established flow zone.

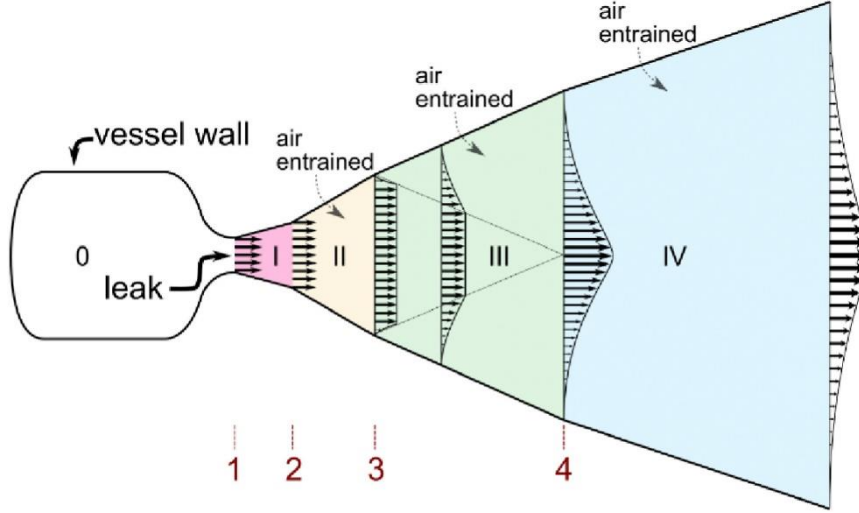


Figure 1. Schematic of an underexpanded jet

In this study, the important thermodynamic states along the flow stream are represented by the numbers 0-4. Both hydrogen and air are assumed to be simple compressible substances in thermodynamic equilibrium, and the hydrogen is stagnant in the tank. Considering the condensation effect of the different air components, the air was assumed to be a simple mixture consisting of 78% nitrogen and 22% oxygen.

For the  $C_2H_2$  stored at station 0, assuming its thermodynamic state is known, the state and mass flow rate of hydrogen at station 1 is determined from the isentropic process and the orifice diameter. High momentum flow through Zone I is assumed to expand into ambient pressure, thus the exit flow from Zone I is consistent with the subsonic jet law. Starting from Zone II, the air is entrained into the jet area. Considering the possibility of condensation of the entrained air, the multiphase flow equilibrium momentum equation and energy equation are added to the fully turbulent and quasi-steady flow in Zone II. The flow in Zone III is no longer a plug flow, and a radial variation of the jet flow characteristics is achieved. Zone IV describes the jet trajectory by solving the differential conservation equations for mass, momentum, hydrogen concentration and energy. More details on the integral model can be found in the reference [27].

## 2.2 Underexpanded Zone (Zone I)

Underexpanded jets generated by high-pressure hydrogen at the real orifice are usually accompanied by complex shock structures. The underexpanded jets need to be simplified as low-pressure leakage problems to provide equivalent boundary conditions for the overall integral model. Several notional nozzle models have been developed to calculate the thermodynamic state of the underexpanded jet after the complex shock structure [15-19], with each model conserving mass between flow through the real orifice and flow through the notional nozzle, and the pressure of station 2 is equal to the ambient pressure.

The notional nozzle model of Brich et al. (1987) [16] is used to determine the effective diameter and velocity of station 2 in this study. The mass conservation and momentum conservation equations of Zone I are shown in Eqs. (1)-(2). The exiting temperature of the notional nozzle is assumed same as the stagnant gas temperature, the density of hydrogen at the exit of the notional nozzle is obtained by the COOLPROP database in Eq (3).

$$V_2 = V_1 + \frac{P_1 - P_{amb}}{\rho_1 V_1} \quad (1)$$

$$A_2 = \frac{\rho_1 V_1^2 A_1}{\rho_2 (P_1 - P_{\text{amb}} + \rho_1 V_1^2)} \quad (2)$$

$$\rho_2 = \rho(T_0, P_{\text{amb}}) \quad (3)$$

where  $V$  is the jet velocity,  $P$  is the jet pressure,  $\rho$  is the jet density,  $A$  is the orifice area,  $h_{\text{amb}}$  is the ambient enthalpy,  $T$  is the jet temperature.

### 2.3 Initial entrainment and heating Zone (Zone II)

The initial entrainment and heating zone (Zone II) is the focus of this study. Previous models have assumed that the minimum temperature at the exit of zone II is that the hydrogen and air mixture will maintain a gaseous state, which may be seriously inconsistent with reality. In the HyRAM model [26], this region is directly ignored due to its short length of this region. In fact, the temperature in the flow core area leaving Zone I is much lower than the ambient temperature. When a pure hydrogen stream entrains the surrounding ambient air, the nitrogen, oxygen and water vapor in the air may condense or even freeze, therefore the mixture cannot be characterized by the currently available equilibrium models. In developing the model for Zone II, the following assumptions were used:

- (1) The flow stream is turbulent and quasi-steady;
- (2) Plug flow model is used, the radial turbulent transport occurs only at the periphery of the jet, the radial distribution of velocity, concentration and enthalpy is uniform at any axial position in the jet;
- (3) Buoyancy is neglected due to the initial entrainment and heating zone being short and the trajectory of the jet is not significantly altered as a result of buoyant forces;
- (4) The entire flow field pressure is one atmosphere;
- (5) Only nitrogen condensation is considered;
- (6) The hydrogen and air mixture and possibly liquid phase material are in thermodynamic equilibrium, which has different phase velocities;
- (7) The changes in potential energy are negligible.

Eqs. (4)-(6) illustrates the conservation of mass, momentum and energy of this zone:

$$\dot{m}_2 + \dot{m}_{\text{air}} = \dot{m}_3 + \dot{m}_{\text{LN}_2} \quad (4)$$

$$\dot{m}_2 V_2 = \dot{m}_3 V_3 + \dot{m}_{\text{LN}_2} V_{\text{LN}_2} \quad (5)$$

$$\dot{m}_2 \left( h_2 + \frac{1}{2} V_2^2 \right) + \dot{m}_{\text{air}} h_{\text{air}} = \dot{m}_3 \left( h_3 + \frac{1}{2} V_3^2 \right) + r + \dot{m}_{\text{LN}_2} h_{\text{LN}_2} \quad (6)$$

where  $V_2$  is the velocity of pure hydrogen entering the zone at station 2,  $V_3$  is the velocity of the air-hydrogen mixture exiting the zone at station 3, and  $r$  is latent heat released by nitrogen condensation. The temperature of station 3 ( $T_3$ ) is an assumed value. For the COOLPROP database does not support the characterization of solid nitrogen thermodynamic properties,  $T_3$  can be set to 63.17 K minimum.

The air-hydrogen mixture enthalpy ( $h_3$ ) is determined from the state specified by  $T_3$ , atmospheric pressure and the composition of the exiting by using the COOLPROP database:

$$h_3 = h(T_3, P_{\text{amb}}, Y_3) \quad (7)$$

where  $Y_3$  represents the set of mass fractions for exiting air-hydrogen mixture.

The condensation temperature of nitrogen at atmospheric pressure is 77.35 K, and the solidification temperature is 63.17 K. In this study, condensation of the nitrogen component in air occurs when the temperature of station 2 is below 77.35 K. The mixture at station 3 consists only of hydrogen, oxygen, and nitrogen that has not liquefied. The condensation factor  $\sigma$  is introduced into the model for Zone II to describe the proportion of nitrogen in the exiting air that condenses:

$$\sigma = \frac{T_3 - T_{\text{condensation}}}{T_{\text{condensation}} - T_{\text{solidification}}} \quad (8)$$

The enthalpy, density, velocity, and mass flow rate of Station 3 can be expressed by the following equations:

$$\rho_3 = \frac{1}{\frac{(1 - \sigma \cdot \varphi_{\text{N}_2})(1 - Y_3)}{\rho_{\text{mixture}}} + \frac{Y_3}{\rho_{\text{H}_2}}} \quad (9)$$

$$h_3 = (1 - \sigma \cdot \varphi_{\text{N}_2})(1 - Y_3)\rho_{\text{mixture}} + Y_3 h_{\text{H}_2} \quad (10)$$

$$\dot{m}_3 = \dot{m}_2 + \frac{(1 - \sigma \cdot \varphi_{\text{N}_2})(1 - Y_3)}{Y_3} \dot{m}_2 \quad (11)$$

$$V_3 = \frac{V_2 \dot{m}_3 \rho_2}{\dot{m}_2 \rho_{\text{mixture}}} \quad (12)$$

where  $\varphi_{\text{N}_2}$  is the volume fraction of nitrogen in the  $\text{N}_2$  and  $\text{O}_2$  mixture.  $\rho_{\text{mixture}}$  is the exiting density of the initial reel suction and heating zone, which is evaluated from expressions of the form:

$$\rho_{\text{mixture}} = \varphi_{\text{N}_2} (1 - \sigma)(1 - Y_3)\rho_{\text{N}_2} + (1 - \varphi_{\text{N}_2})(1 - Y_3)\rho_{\text{O}_2} + Y_3 \rho_{\text{H}_2} \quad (13)$$

For cases where the hydrogen temperature at Station 2 exceeds 77.35 K, there is no condensation occurs in Zone II. For most cryogenic hydrogen leaks this very rarely happens. Although the length of Zone II is very short, Figure 2 has shown that directly replacing the Zone II exiting states with the station 2 thermodynamic parameters, which would lead to an overestimation of the station 3 mass fraction. Therefore, considering condensation effects in the Zone II model can provide more accurate boundary conditions for the subsequent integral model.

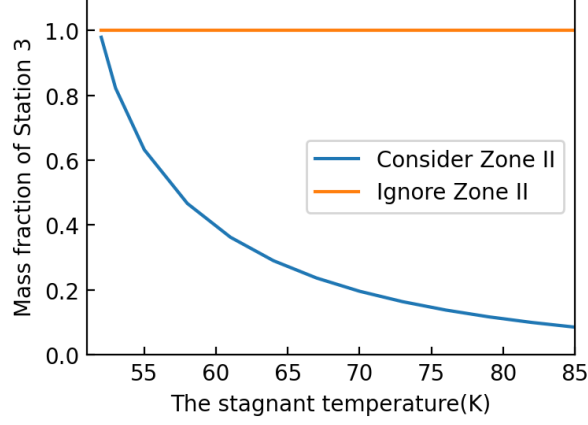


Figure 2. The effect of the zone II model on the mass fraction of station 3

#### 2.4 Flow establishment Zone and Established flow zone (Zone III and Zone IV)

Zone III, "flow establishment zone", provides the transition between the initial entrainment and heating zone and the established flow zone. In this zone, the plug flow transitions to a fully established Gaussian flow pattern of the jet. The parameters such as mixture velocity, density and concentration vary with the jet radius, which on the centerline decreases with increasing distance from the jet centerline. At this zone, the jet gradually changes from momentum-dominated to buoyancy-dominated due to the jet being away from the orifice. The length of Zone III ( $S_E$ ), the characteristic jet width ( $B_E$ ), centerline mass fraction ( $Y_{cl,E}$ ) of station 4 are obtained from the following equations:

$$B_E = \beta_B d_e \quad (14)$$

$$S_E = \beta_S d_e \quad (15)$$

$$Y_{cl,E} = Y_3 \frac{\lambda^2 + 1}{2\lambda^2} \quad (16)$$

where  $\beta_B$  and  $\beta_S$  are empirical coefficients and  $\lambda$  is the relative concentration to velocity spreading ratio. For underexpanded jets,  $\beta_B$  is assumed to be 0.82,  $\beta_S$  is assumed to be 8.632, and  $\lambda$  is 1.529 [20].

Zone IV is the established flow zone, which is the longest region in the integral model. Conservation equations for mass, momentum, hydrogen concentration and energy are given by:

$$\frac{\partial}{\partial S} \int_0^{2\pi} \int_0^{\infty} \rho V r dr d\phi = \rho_{amb} E \quad (17)$$

$$\frac{\partial}{\partial S} \int_0^{2\pi} \int_0^{\infty} \rho V^2 \cos \theta r dr d\phi = 0 \quad (18)$$

$$\frac{\partial}{\partial S} \int_0^{2\pi} \int_0^{\infty} \rho V^2 \sin \theta r dr d\phi = \int_0^{2\pi} \int_0^{\infty} (\rho_{amb} - \rho) g r dr d\phi \quad (19)$$

$$\frac{\partial}{\partial S} \int_0^{2\pi} \int_0^{\infty} \rho V Y r dr d\phi = 0 \quad (20)$$

$$\frac{\partial}{\partial S} \int_0^{2\pi} \int_0^{\infty} V \rho (h - h_{\text{amb}}) r dr d\phi = 0 \quad (21)$$

where  $E$  is the air entrainment,  $h$  is the jet enthalpy,  $Y$  is the hydrogen jet mass fraction,  $g$  is gravitational constant.  $x$  and  $z$  are the horizontal and vertical coordinates of the jet centerline,  $S$  is the streamline coordinate along the jet centerline (also denoted by  $z$  for a vertical jet),  $r$  is the radial distance from the jet centerline,  $\theta$  is the angle between the streamline direction and the horizontal.

Previous studies [27,28] have shown that within the established flow zone, the jet velocity, density and hydrogen mass fraction follow a Gaussian distribution in the radial direction:

$$V = V_{\text{cl}} \exp(-r^2 / B^2) \quad (22)$$

$$\rho - \rho_{\text{amb}} = (\rho_{\text{cl}} - \rho_{\text{amb}}) \exp\left(\frac{-r^2}{\lambda^2 B^2}\right) \quad (23)$$

$$\rho Y = \rho_{\text{cl}} Y_{\text{cl}} \exp\left(\frac{-r^2}{\lambda^2 B^2}\right) \quad (24)$$

where  $V_{\text{cl}}$  is the local centerline velocity,  $B$  is the characteristic jet width or the radial distance at which  $V$  is equal to  $1/e$  times  $V_{\text{cl}}$ ,  $\rho_{\text{cl}}$  is local centerline density,  $Y_{\text{cl}}$  is the local centerline hydrogen mass fraction.

### 3.0 RESULTS

Li et al. [25] measured the time-averaged concentration and temperature data of  $\text{C}_2\text{H}_2$  jets by using laser Raman scattering diagnostics. The  $\text{C}_2\text{H}_2$  were released from a liquid hydrogen source through 1 mm and 1.25 mm diameter orifices at back pressures ranging from 2 to 6 bar. Figure 3 shows the predicted results from the integral model as compared to the data from the cryogenic compressed hydrogen experiments for a vertical jet. The integral model is found to be in excellent agreement with the  $\text{C}_2\text{H}_2$  jet data. The model can accurately reproduce the mole fraction decay along the centerline.

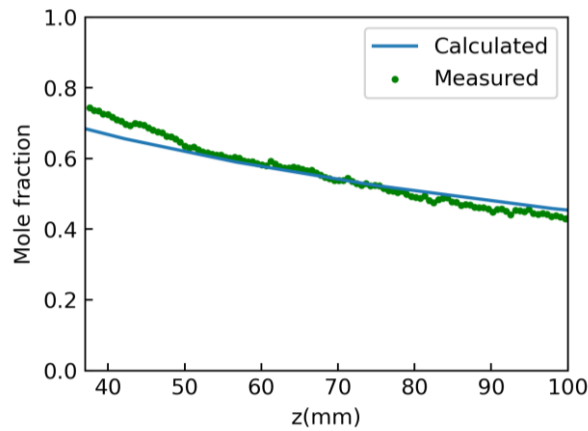


Figure 3. Measured and calculated mean mole fraction for hydrogen mole fraction along the jet centerline (orifice diameter =1.25 mm, 3 bar, 51 K)

Figure 4 shows the predicted and measured mean concentration fields for underexpanded jets with a nozzle diameter of 1.25 mm for cryogenic hydrogen (3 bar, 51 K). The subfigures on the right were obtained from Ref. [25]. The model successfully reproduced the concentration field for the whole measurement range. In the area away from the axis, the model slightly overpredicted the mole fraction.

The radial mole fraction distributions at different axial locations are shown in Figure 5. The radial molar fraction distributions at different axial locations. Although the centerline molar fractions (the peak concentrations on each curve) are in good agreement, the radial profiles predicted by the integral model were wider than the experimental data. Therefore, the empirical coefficients of the room-temperature hydrogen experimental data may no longer be suitable for the CcH<sub>2</sub> jet. Future work will require further fitting of the empirical coefficients using a large amount of experimental data.

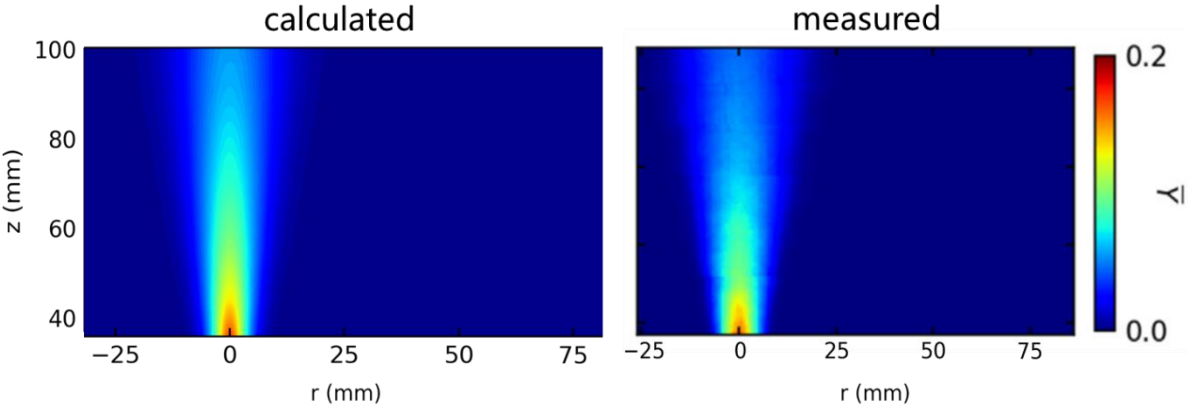


Figure 4. Measured and calculated mean mole fraction for hydrogen mole fraction for cryogenic compressed hydrogen (orifice diameter = 1.25 mm, 3 bar, 51 K)

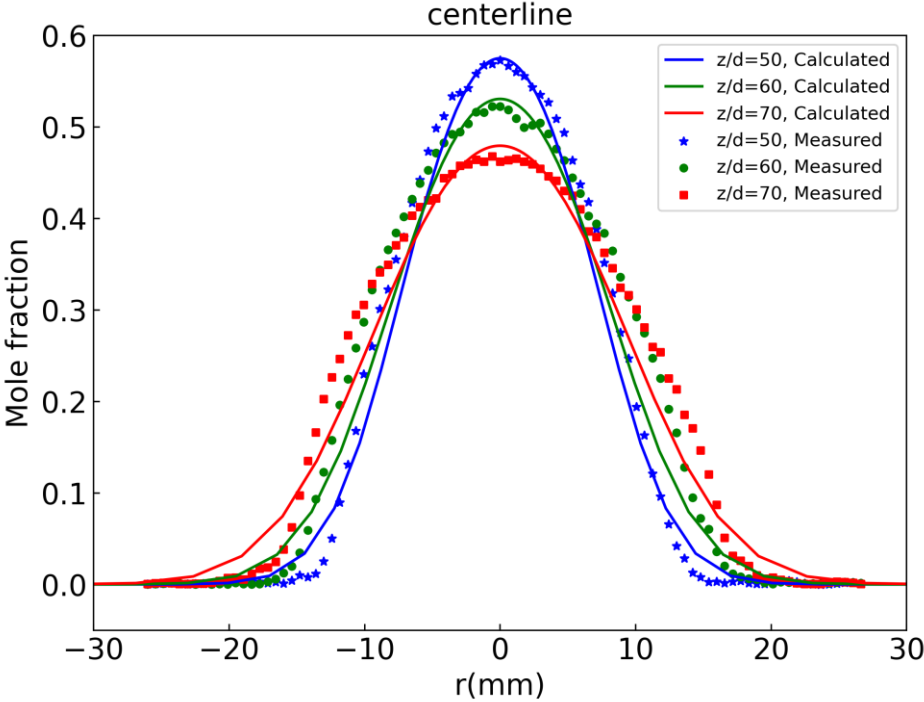


Figure 5. The radial molar fraction distributions at different axial locations

## 4.0 CONCLUSIONS

The study developed an integral model of the cryogenic hydrogen jet considering the condensation of the air components. The integral model includes the initial entrainment and heating zones which were not considered in previous models. The predicted results were compared with the experimental data. The results show that the model considering the air component condensation can accurately predict the cryogenic hydrogen jet trajectories and concentration distributions. The model successfully calculated the concentration fields for the whole measurement range. In the area away from the axis, the model slightly overpredicted the mole fractions. Therefore, the empirical coefficients of the room-temperature hydrogen experimental data may no longer be suitable for the CcH<sub>2</sub> jet. The integral model is a promising tool for fast, accurate predictions of the flow fields of CcH<sub>2</sub> jets. In the future work, the condensation of oxygen and water vapor will also be considered, the empirical coefficients will be improved by using a large amount of experimental data for more accurate predictions.

## REFERENCES

1. Barbir F., Transition to Renewable Energy Systems with Hydrogen as an Energy Carrier. *Energy*, **34**, No. 3, 2009, pp. 308-312.
2. Apak S., Atay E., Tuncer G., Renewable Hydrogen Energy and Energy Efficiency in Turkey in the 21<sup>st</sup> Century. *International Journal of Hydrogen Energy*, **42**, No. 4, 2017, pp. 2446-2452.
3. DOE National Clean Hydrogen Strategy and Roadmap, U.S. Department of Energy, 2022. <https://www.hydrogen.energy.gov/pdfs/clean-hydrogen-strategy-roadmap.pdf>
4. Natalia G., Future of Renewable and Low-Carbon Hydrogen in Europe, Stratas Advisors, 2020.
5. Ding M., Characteristics, Motivation, International Coordination of Japan's Hydrogen Strategy, *Contemporary Economy of Japan*. No. 4, 2021, pp. 28-41(in Chinese).
6. Schefer R.W., Houf W.G., Williams T.C., Investigation of Small-scale Unintended Releases of Hydrogen: Buoyancy Effects. *International Journal of Hydrogen Energy*, **33**, No. 17, 2008, pp. 4702-4712.
7. Ruggles A.J., Ekoto I.W., Ignitability and Mixing of Underexpanded Hydrogen Jets. *International Journal of Hydrogen Energy*, **37**, No. 22, 2012, pp. 17549-17560.
8. Saffers J.B., Molkov V.V., Towards Hydrogen Safety Engineering for Reacting and Non-reacting Hydrogen Releases. *Journal of Loss Prevention in the Process Industries*, **26**, No. 2, 2013, pp. 344-350.
9. Takeno K., Okabayashi K., Kouchi A., Misaka N., Hashiguchi K., Concentration Fluctuation and Ignition Characteristics During Atmospheric Diffusion of Hydrogen Spouted from High Pressure Storage, *International Journal of Hydrogen Energy*, **42**, No. 22, 2017, pp. 15426-15434.
10. Abraham G., Horizontal Jets in Stagnant Fluid of Other Density, *Journal of the Hydraulics Division*, **91**, No. 4, 1965, pp. 139-154.
11. Gebhart B., Hilder D.S., Kelleher M., The Diffusion of Turbulent Buoyant Jets. *Advances in heat transfer*, **16**, 1984, pp. 1-57.
12. Houf W., Schefer R., Analytical and Experimental Investigation of Small-scale Unintended Releases of Hydrogen, *International Journal of Hydrogen Energy*, **33**, No. 4, 2008, pp. 1435-1444.
13. El-Amin M.F., Kanayama H., Similarity Consideration of the Buoyant Jet Resulting from Hydrogen Leakage. *International Journal of Hydrogen Energy*, **34**, No. 14, 2009, pp. 5803-5809.
14. Xiao J., Travis J.R., Breitung W., Non-Boussinesq Integral Model for Horizontal Turbulent Buoyant Round Jets. *Science & Technology of Nuclear Installations*, **1**, 2009, pp. 1-7.
15. Birch A.D., Brown D.R., Dodson M.G., et al. The Structure and Concentration Decay of High Pressure Jets of Natural Gas, *Combustion Science & Technology*, **36**, No. 5-6, 1984, pp. 249-261.
16. Birch A.D., Hughes D.J., Swaffield F., Velocity Decay of High Pressure Jets. *Combustion Science & Technology*, **52**, No. 1-3, 1987, pp. 161-171.

17. Ewan B.M.K., Structure and Velocity Measurements in Underexpanded Jets, *Combustion Science and Technology*, **45**, No. 5-6, 1986, pp.275-288.
18. Yuceil K., Otugen M., Scaling Parameters for Underexpanded Sonic Jets. *Physics of Fluids*, **14**, No. 12, 2002, pp.4206-4215.
19. Molkov V., Fundamentals of Hydrogen Safety Engineering II. E Book at Bookboon Com, 2012.
20. Li X., Hecht E.S., Christopher D.M., Validation of a Reduced-order Jet Model for Subsonic and Underexpanded Hydrogen Jets. *International Journal of Hydrogen Energy*, **41**, No. 2, 2016, pp.1348-1358.
21. Friedrich A., Breitung W., Stern G., Vesper A., Kuznetsov M., Fast G., Ignition and Heat Radiation of Cryogenic Hydrogen Jets. *International Journal of Hydrogen Energy*, **37**, No. 22, 2012, pp.17589-17598.
22. Hecht E.S., Panda P.P., Mixing and Warming of Cryogenic Hydrogen Releases. *International Journal of Hydrogen Energy*, **44**, No. 17, 2019, pp. 8960-8970.
23. Ba Q., He Q., Zhou B., Chen M., Li X., Cheng L., Modeling of Cryogenic Hydrogen Releases. *International Journal of Hydrogen Energy*, **45**, No. 55, 2020, pp.31315-31326.
24. Giannissi S.G., Venetsanos A.G., Hecht E.S., Numerical Predictions of Cryogenic Hydrogen Vertical Jets. *International Journal of Hydrogen Energy*, **46**, No. 23, 2020, pp. 12566-12576.
25. Li X., Yao C., Egbert S.C., He Q., Zhao Z., Christopher D.M., and Hecht E.S., Self-similar Characteristics of Underexpanded, Cryogenic Hydrogen and Methane Jets. *International Journal of Hydrogen Energy*, **48**, No. 10, 2023, pp. 4104-4117.
26. Groth K.M. and Hecht E.S., HyRAM: a Methodology and Toolkit for Quantitative Risk Assessment of Hydrogen Systems, *International Journal of Hydrogen Energy*, **42**, No. 11, 2017, pp. 7485-7493.
27. Houf W.G. and Winters W.S., Simulation of High-pressure Liquid Hydrogen Releases, *International Journal of Hydrogen Energy*, **38**, No. 19, 2013, pp. 8092-8099.
28. Winters W.S. and Houf W.G., Simulation of Small-scale Releases from Liquid Hydrogen Storage Systems, *International Journal of Hydrogen Energy*, **36**, No. 6, 2011, pp. 3913-3921.